

Modelling of powder die compaction for press cycle optimization

Jean-Philippe Bayle^{1,*}, Vincent Reynaud², François Gobin¹, Christophe Brenneis¹, Eric Tronche¹, Cécile Ferry¹, and Vincent Royet¹

¹ CEA, DEN, DTEC, SDTC, 30207 Bagnols/Cèze, France

² Champalle Company, 151 rue Ampère, ZI Les Bruyères, 01960 Peronnas, France

Received: 21 September 2015 / Received in final form: 16 February 2016 / Accepted: 15 March 2016
Published online: 13 May 2016

Abstract. A new electromechanical press for fuel pellet manufacturing was built last year in partnership between CEA-Marcoule and Champalle^{Alcen}. This press was developed to shape pellets in a hot cell via remote handling. It has been qualified to show its robustness and to optimize the compaction cycle, thus obtaining a better sintered pellet profile and limiting damage. We will show you how 400 annular pellets have been produced with good geometry's parameters, based on press settings management. These results are according to a good phenomenological pressing knowledge with Finite Element Modeling calculation. Therefore, during die pressing, a modification in the punch displacement sequence induces fluctuation in the axial distribution of frictional forces. The green pellet stress and density gradients are based on these frictional forces between powder and tool, and between grains in the powder, influencing the shape of the pellet after sintering. The pellet shape and diameter tolerances must be minimized to avoid the need for grinding operations. To find the best parameters for the press settings, which enable optimization, FEM calculations were used and different compaction models compared to give the best calculation/physical trial comparisons. These simulations were then used to predict the impact of different parameters when there is a change in the type of powder and the pellet size, or when the behavior of the press changes during the compaction time. In 2016, it is planned to set up the press in a glove box for UO₂ manufacturing qualification based on our simulation methodology, before actual hot cell trials in the future.

1 Introduction

The electronuclear closed fuel cycle chosen by France plans the reprocessing of spent fuel and will enable natural uranium resource saving, as well as a reduction in the volume of wastes and their toxicity compared with the choice of direct storage (once-through cycle). The nuclear waste from spent fuel is classified depending on its activity and half-life. The High Activity (HA) waste represents more than 95% of the total radioactivity of French nuclear waste. The liquid extraction process called PUREX enables the Minor Actinides (MAs) to be separated from the Fission Products (FP) in HA waste. The advanced management of the MAs is a goal for the transmutation envisaged in fourth generation reactors or in specially-dedicated reactors. Two approaches to MA transmutation in fast breeder reactors (FBRs) are envisaged, i.e. homogeneous and heterogeneous recycling. The heterogeneous mode consists in concentrating the MAs in special assemblies located in the periphery of the reactor core. The neutronic impact on the core limits the introduction of a higher quantity of MAs, restricted to 10 to

20%. Materials including Americium (Am) located around the reactor core can be of target type if the MA supports an inert matrix, or else part of a Minor Actinide Bearing Blanket (MABB) if the MAs are directly incorporated into fertile UO₂ fuels.

2 Context

The manufacturing of fuel pellets incorporating minor actinides by remote handling in hot cells requires simple, effective operations and robust technologies. Rejects must be minimized, which is harder with higher and higher actinide concentrations. The process of pellet shaping is well known from the literature [1–4]. It is generally carried out by uniaxial cold compaction in die to obtain green pellets (rough pellets from the pressing) with a density of about 65% of the theoretical density (th.d). This shaping is then followed by a sintering operation which enables the density to reach 95% of the th.d. At present, the pressing technology used in Atalante hot cells (Marcoule, France) is based on a manual process with a radial opening die, compared to the conventional process of a floating die

* e-mail: jean-philippe.bayle@cea.fr.

where a downward movement of the die occurs, enabling the ejection of the pellet. Another process with a fixed die enables pellet ejection by the lower punch which pushes with a pressure support from the upper punch. Damages can be present after the ejection stage if the pressure from the two punches is not coordinated, and these are generally revealed during the sintering stage. They can be worsened by the radiological behavior of the pellet, depending on its composition, and by the manufacturing process. Different defect types occur for sintered pellets, in particular cracks, end-capping and spalling [5]. Cracks can form down the sides of pellets and be longitudinal or lateral, or happen in the ends and sometimes cause “end capping” in the top or bottom of the pellets. Spalling can be found on the sides or the ends. The green pellets can have defects which depend essentially on the level of support pressure during die ejection. Other sources of damage can also be identified in the process of powder shaping [6]. First, the introduction of secondary phases composed of hard inclusions or air pockets leads to an excessive relaxation during ejection, with spalling occurring on the pellets, and to different wear patterns on the internal walls of the die and thus to blocked pellet sliding and to shearing. Secondly, inappropriate press settings for compression level, pressing time, or punch accompanying pressure during ejection can cause damage.

The mechanical stress distribution within pellets during the ejection step influences the surface defects. The mechanical stress induced by the die can be high, in particular at the corner of the die, where the springback occurs during the pellet ejection. The stress concentrations are accentuated by springback, which corresponds to the volume expansion of the pellet by relaxation of stress during ejection. Some authors have used digital simulation to estimate the mechanical stresses in pellets during this step. Aydin and Briscoe [1] attempted to determine the residual stress distributions in cylindrical pellets. Their study showed that axial residual tensile stress appears at the extremities of the pellet from the axial stress relaxation stage in die (decompression in die). These stresses are due to the friction forces between the die and the pellet, which block the axial springback when the pressure is released. In their study, neither the pellet slide and release phase nor the interactions with the edge of the die were taken into account, as the radial walls of the die were artificially removed. Jonsen and Haggblad [7] took into account the compaction and the ejection with the real kinematics of ejection. The distribution of the residual stress consolidated by measurements of neutron diffraction shows that the pellet edges are submitted to axial compression over a thin layer (200–400 μm), and the part below this layer undergoes traction over a thicker zone (600 μm). From these two studies, it is known that residual stresses after ejection are strongly influenced by the tool shapes and kinematics of ejection. In this context, an ejection performed by a radial die opening is expected to be less damaging. Therefore, this mode of ejection was used for the manufacturing of the minor actinide fuel pellets considered in this study.

Another issue is that minor actinide fuel pellet grinding after sintering must be minimized in order to limit highly radioactive dust. Consequently, geometrical tolerance for the diameter needs to be rather wide, $\pm 50 \mu\text{m}$ around

nominal values (8–10 mm). Pellet geometrical dimension mastery is necessary in order to obtain “net shape” pellets. It is well known that the pressing stage is critical for the shape of the pellet after sintering. For instance, when uniaxial compaction is performed green densities decrease along the height of the compact from the extremity which was in contact with the moving punch. After sintering, the shrinkage follows the density gradient and a conical shaped pellet is formed. With two mobile punches, a double-conical (hourglass) shaped pellet is obtained. In die compression, the heterogeneous density is due to the friction forces between the powder and the wall of the die, as well as the friction between the grains of the powder [1,8]. These friction effects have been extensively studied for perfectly cylindrical dies, but never investigated for a specially shaped die. More particularly, the diametrical profile of the die could be designed in order to counterbalance the effect of friction.

3 Objectives

The density gradients obtained in the compact depends on various parameters such as the tool quality, the powder behavior, the compaction cycles, the lubrication type, etc. Because the powders used for nuclear fuel manufacturing are precious, pellet damage must be minimized and a net-shaped pellet is necessary because it does not require grinding. The main objective of this study was to be able to anticipate the demanding manufacturing factors, which can influence the press settings before the production cycle, and then during the manufacturing, to be able to have the shortest possible response time to correct parameters to ensure finished products with stable quality. Consequently, the study firstly concerned the optimization of the fuel manufacturing cycles of an innovative nuclearized press for nuclear fuel manufacturing in a hostile and restricted environment. To meet this need, a capability study of the press is described, with on the first press regulation results in the inactive conditions of a mock-up. An annular geometry pellet with compulsory manufacturing tolerances is taken into account. From the results of the study, simulations are proposed on the basis of previous simulations where the model parameters of the compaction were characterized for various powders. We can thus act on the cycle compaction parameters of the press, on the model parameters of each powder, and on certain friction coefficients depending on the lubricant type.

4 Materials and methods

4.1 Alumina powder (Al_2O_3 _ T195)

Alumina powder was used in this study. Its behavior is known from the literature [4], and it is widely used in the compaction field. Alumina powder was used to guarantee the conformity of the measurement and calculation results which could be compared with those from unpublished works [3]. Furthermore, it will be used to carry out

Table 1. Characteristics of Al_2O_3 powder.

Powder	Supplier	Morphology	Size (μm)	Bulk density ($\text{g}\cdot\text{cm}^{-3}$)	Theoretical density ($\text{g}\cdot\text{cm}^{-3}$)	E_{Th} Theoretical Young's modulus (GPa)	ν_{Th} Theoretical Poisson's ratio
Al_2O_3	Ceraquest	Spherical	50–200	1.24	3.970	530	0.22

qualification trials for a new nuclearized press currently undergoing testing. The particles are spherical, 50 to 200 μm in diameter. These spheres in turn are composed of 1–10 μm grains [9]. Main characteristics of studied Al_2O_3 powder are summarized in Table 1.

4.2 New nuclear press description and characteristics

One of the fuel manufacturing processes originates in the conventional process of the powder metallurgy industry and enables pellet shaping in dies, followed by sintering. The shaping of the Minor Actinide Bearing Blanket (MABB) pellets is currently done manually in hot cells. Manufacturing Automation and a better control of the shaping parameters were tested during this study, in order to prepare the way for a new automatic nuclear press under a collaboration set up between the CEA and Champalle^{Alcen}. The minimization of criticality risks is an important goal for MABB pellet manufacturing, and is the main reason why the press is being built to operate without oil, and is completely electromechanical. It is a uniaxial automatic mono-punch simple effect press, with a displacement-piloted die. Its capacity is 10 tons, the maximum height is limited to 1.2 m and the production rate is one to five cylindrical annular pellets per minute. Installing the apparatus in an existing hot cell for nuclear fuel production required a modular design and simulation studies, which were carried out using 3D software to show the entry of all modules through the airlock. The objective was to validate the modular units' ability to be assembled, dismantled and maintained by remote handling techniques. The 30 separate units making up the press had to go through a 240 mm diameter air-lock to enter the hot cell. To be sure the remote handling scenarios were appropriate, virtual reality simulation studies were carried out, taking into account force feedback and inter-connectability between the different units [10,11]. In parallel, different radiological software checked that the press components' radiological dimensioning would ensure radiation resistance during operation in a hostile environment. A mock-up simulating the future hot cell and equipped with the real remote handling systems has been built in the CEA/Marcoule HERA facility technological platform, in order to physically test press unit assembly by remote handling, and the apparatus operations. The press, adapted to nuclear conditions, is patented. The press is a uniaxial mono-punch press, with a single compaction cycle. The upper punch and die are mobile at different velocities and the lower punch is fixed. The die is used for the ejection step with an upper punch pressure support. The hot cell press location imposed

the use of an existing hot cell, without modifications or external motors being possible. A transfer of the module units through the 240 mm diameter of the Lacalene Leaktight Transfer Double Door had to be carried out. To minimize the criticality impact and because hydrogenated liquids are prohibited in hot cell, we replaced hydraulic energy by electric energy. This is the main reason why the choice was made of electric motors with transmission systems with a minimum gap, combining rotary and translatory mechanisms for the upper punch and the die. To decrease the height needed, the die motorization was placed to one side and the effort transmitted via a toggle joint to the die plate. The press production rate is about four pellets per minute and its pressure capacity is 10 tons. The base structure has one lower plate. This plate is fixed to a circular rail built into the hot cell floor. The press can therefore be rotated in order to enable access to any of the five main parts as required. The first part includes the rigid frame of the press, consisting of the lower and upper plates connected by four guide columns. The plates support respectively the motors of the die and of the upper punch. The lower plate holds the fixed lower punch equipped with a displacement sensor. Between these two plates, the upper punch and the die plates (parts 2 and 3) slide up and down. Plate displacements are monitored by sensors, and the mobile upper punch is also fitted with a force sensor. The powder load system and displacement motor of the filling shoe are set up on the mobile die plate. The filling shoe is moved laterally by an electric motor and a rack system. The powder load system has a tippable powder transfer jar which can be completely connected using remote handling. The press was patented under a CEA and Champalle common patent [12]. The nuclear press has enabled the manufacturing of Al_2O_3 annular pellets with a 10 mm die diameter in CEA Marcoule mock-up. The Al_2O_3 powder was used, with zinc stearate lubrication in the mass measured at 2%.

4.3 Optimization cycle background

The use of the press with slave die displacement (equivalent to a double effect cycle) can enable cycle optimization and operating, in order to reduce the difference between the minimum and maximum pellet diameters. An optimal operating cycle enabling uniform stress distribution throughout the pellet means making the applied and transmitted forces equivalent. The difference between these forces is called Δ . To influence Δ , several parameters were varied in the compaction cycle. Figure 1 shows the upper, applied and lower transmitted punch forces, die and upper

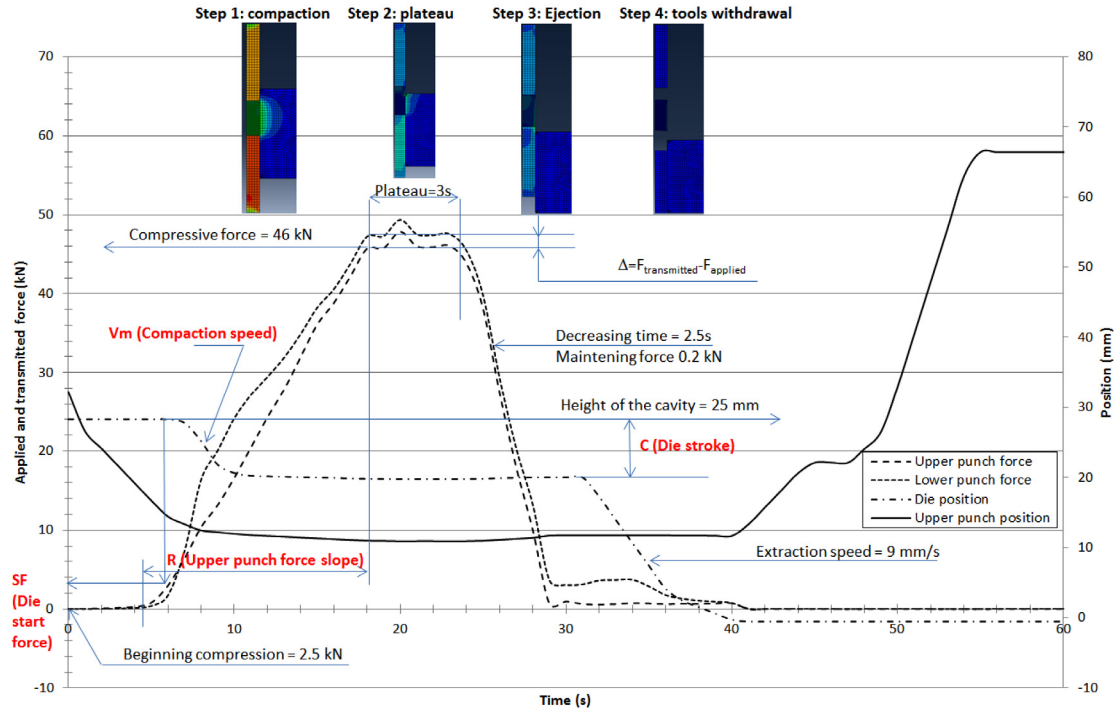


Fig. 1. Upper, applied and lower transmitted punch forces, die and upper punch displacements depending on time, Von Mises stresses during step calculations (1 to 4), corresponding to the compaction cycle.

Table 2. Regulation parameters of the cycle press, SF , R , C , V_m .

Parameters	Symbol	Value	Unit
Die start force	SF	3.5	kN
Upper punch force slope	R	5	s
Die stroke	C	6	mm
Die compaction speed	V_m	7	mm/s

punch displacements depending on time. The compaction cycle settings for a given powder thus require an optimization of the press setting parameters.

For the Al_2O_3 powder studied, in order to obtain a geometrical tolerance of ± 0.012 mm for a diameter sintered to 9.015 mm, the chosen parameters are indicated in Table 2. For R , it is the time to increase from 3.5 to 46 kN. Parameter C is equal to the difference between the position of the height of the powder column (25 mm) and the position of the compression start point (19 mm) which enables a green pellet height to be compacted to 11 mm.

Constants are: the force at the beginning of compression is set (punch) at 2.5 kN; the compressive force (punch) is 46 kN; time to the compression plateau (punch) is 3 s; the decreasing slope (punch) is set at 2.5; the maintaining force (punch) at 0.2 kN; the position of the height of the cavity (die) at 25 mm; the extraction speed is set (die) at 9 mm/s. For the Al_2O_3 powder studied, we obtained a geometrical

tolerance of ± 0.012 mm for a diameter sintered to 9.015 mm. The die diameter was of 10.000 mm. These optimal settings meant the best pellet quality was obtained, with a lubricant inside the powder and with a good flowing powder. To summarize, to minimize Δ , you must find a compromise between V_m and R in order to reduce the friction index depending on the flow index (powder behavior) and the friction coefficient (powder and die friction) [9].

5 Modelling

5.1 Model description

Roscoe et al. of Cambridge University first established general relationships of soil behavior based on the theory of elastoplasticity with strain hardening, in the field now described by Cam-Clay (CC) Model. These models are based on four main elements: the study of isotropic compression tests, the concept of critical state, a force relation-dilatancy and the rule of normality for plastic strain. In the CC model, the elliptical load surface (plastic potential), in isodensity, is defined in the plan of invariants (P, Q) by the expression below [2,4,8,13]:

$$f(P, Q, \rho(\varepsilon_V^P)) = (Q/M)^2 + P(P - P_C) = 0,$$

- $P = (\sigma_{Applied} + 2\sigma_{Radial})/3$, hydrostatic stress (MPa),
- $Q = |\sigma_{Applied} - \sigma_{Radial}|$, deviatoric stress (MPa),

- $M = \phi(\beta, \mu, \sigma_{\text{Applied}}, \sigma_{\text{Transmitted}}, \sigma_{\text{Radial}})$, critical state stress (de-densification/densification),
- $P_C(\varepsilon_V^P) = [(P_0 + Cohe) \times e^{-k\varepsilon_V^P}] - Cohe$, consolidation pressure (MPa),
 - $Cohe$, powder cohesion pressure (MPa),
 - P_0 , the initial consolidation pressure (MPa),
 - ε_V^P is the plastic volumetric strain with ($\rho = \rho_0 * e^{-\varepsilon_V^P}$, ρ_0 is the initial density),
 - $k = \frac{(1+\varepsilon_0)}{(\text{Lambda}+\text{Kappa})} = \varphi(\sigma_Z, M, \beta, \rho_c, \rho_{ref})$,
 - $\varepsilon_0 = (1 - \rho_{ref})/\rho_{ref}$, void ratio with ($\rho_{ref} = \rho_{real}/\rho_{theo}$),
 - $\sigma_Z(h_{Sensor})$, axial stress at height of the radial sensor (Janssen model),
 - $\beta = \sigma_{Radial}/\sigma_Z(h_{Sensor})$, Flow index,
 - $\rho_c = \rho_{ch} \times \exp(-3\sigma_Z/(1-2\nu)E)$,
 - Lambda = plastic contribution,
 - Kappa = elastic contribution (takes to the oedometric test),
 - E, ν , Young modulus and Poisson coefficients depending on $\beta, \varepsilon_{Vol}, \varepsilon_{Diam}, \sigma$.

In this model, we can choose to use the plastic strain, or density, we preferred to pilot model by the strain hardening variable. The plastic flow occurs when the state of stress meets the condition $f = 0$.

5.2 Model parameter identifications

To determine the $\sigma_{\text{Applied}}, \sigma_{\text{Transmitted}}$ and σ_{Radial} , we used instrumented INSTRON[®] press with upper, lower and radial sensors (strain gauges include in the carbide die). The Jansen model enables the calculation of the axial stress at the level height of the pellet, where the radial strain is measured. Then, we calculated the flow index β (friction in the powder) with the ratio between the radial and axial stresses to the level of the sensor. Also, we calculated with these measures Q and P . Then, we identified elastic (E, ν, Kappa) and plastic coefficients (M, k and Lambda) [14]. Finally, we calculated P_c and the behavior between P and Q depending on the volumetric plastic strain, or density. It is possible to determine Kappa and Lambda without k formulation with the isotropic (oedometric) compression tests. In these, the powder is compacted in a die and then changes in powder height H are drawn up as a function of the applied pressure P . Next, the void ratio is drawn up as a function of the P logarithm with: $e = n/(1 - n)$, where $n = 1 - \rho/\rho_{theo}$ is the powder porosity. The isotropic compression test results give curves $e = f(\ln\sigma)$ which can be considered as lines, a blank consolidation curve, called the Lambda curve, which describes the load during the test and an unloading-reloading curve, called the kappa curve, which describes the non-linear elastic behavior during the test. Another method proposed by Abaqus[®] consists to take into account the tabulation of the curve P_c depending on ε_V^P based on oedometric test [15]. For CC model, we identified coefficients for two powders, Al_2O_3 reference powder (atomized powder) and Ceria powder (microsphere powder) synthesized by WAR process [9].

5.3 Another model

During the calculations with CC model, we observed convergence problems during the first calculations, because of the raw curve considerations stemming from the press data acquisition concerning the upper punch load evolution of force as well as the die and needle displacements. This problem was solved by separating compaction and accompaniment into several steps, so as to soften the slope changes. Another problem of convergence comes from the CC model itself, because it cannot represent a tensile stress (no section of the load surface corresponding to the negative hydrostatic pressures). There is thus a 10% failure of convergence in elastic return. Furthermore, when you draw up Q depending on P , we observed that the first part of the load surface corresponds to a softening ellipse. Rather than implementing this special feature in the initial model like previous Cast3 m[®] study [4,16], we opted for a better adapted Drucker-Prager type model. A Drucker-Prager Cap model (DPC) was tried and compared to CC Model. DPC takes into account the powder cohesion, the linear elasticity or non-linear porous elasticity. It used two main yield surface segments, a linearly pressure dependent DPC shear failure surface: $F_S = t - p \tan\beta - d = 0$.

The cap yield surface: $F_C = \sqrt{(P - P_a)^2 + [Rt/(1 + \alpha - \alpha/\cos\beta)]^2} + R(d + P_a \tan\beta) = 0$ and the transition surface: $F_t = \sqrt{(P - P_a)^2} + [t - (1 - \alpha/\cos\beta)(d + P_a \tan\beta)]^2 - \alpha(d + P_a \tan\beta) = 0$.

All parameters are given in references [2,15].

5.4 Finite element simulations

The geometrical model is an axisymmetric 2D type. It is established based on the powder column, the die and the lower and upper punch. The upper punch and the die are mobile. A connector (equation between two nodes) was used to ensure the speed ratio between the upper punch and the die (punch with rigid connection for piloting via a reference node).

The punch mesh is relatively large and uniform. That of the powder is also uniform, and a little finer. On the other hand, that of the die is much more refined, in particular at the rounded corners in touch with the powder where the stress concentrations are situated, and where the generation of residual stress can be high during the pellet ejection springback. It is the sensitive point which must be handled carefully to avoid generating problems of convergence during the calculation.

During the simulation, the uniaxial simple effect cycle of shaping with a floating die is composed of a succession of discrete stages, each run in a succession of iterations. At the beginning of the calculation, the die is considered to be full of powder, with the upper punch in contact with the powder. At this stage, there is the first step which consists in powder compaction with the upper punch at the speed of 14 mm/s while exercising a push with the die in the same



Fig. 2. Press in the mock-up, with conveyor and tubular container of 37 pellets.

direction as the upper punch but at a more moderate speed, i.e. 10 mm/s. The step is finished when a plateau of a few seconds is reached at 47 kN (600 MPa). The second step consists in pellet ejection by a vertical die withdrawal and the preservation of a support pressure fixed at 11 kN (150 MPa). During this stage, pellet radial springback takes place. The third step consists in withdrawal of the upper punch and complete pellet freeing, when the pellet axial springback occurs. The final step involves the sintering process, and creates shrinkage depending on the density gradients generated during the shaping.

For the press contact elements, the model used is based on the non-penetration of the two bodies in contact. Abaqus[®] uses the Lagrange multipliers method. The algorithm imposes the non-penetration condition on the resolution system by adding unknowns to the system. This greatly increases calculation time. The friction is defined as a Coulomb friction. The Coulomb coefficient taken into account in the calculation is equal to 0.094.

As indicated in reference [13], we used a simple sintering model based on thermal strain to one dimension $\alpha \Delta T = \epsilon_{th}$, with $\alpha = (\rho_c / 95\% \rho_{th})^{1/3} - 1$. To summarize, for each meshing element of the powder, the green density ρ_c was calculated with the Cam-Clay model as well as the corresponding α coefficient. Next, the thermal dilation model of the green density map, the α coefficient map and a temperature level ($\Delta T = 1$) were entered. Shrinkage was thus calculated. A subroutine was developed in a Python language in the Abaqus[®] code to take the sintering step into account [17].

6 Comparisons and discussions

To highlight the best comparison between experimentations and simulations, we have chosen to take into account the capability study realized with the electromechanical

press. Capability machine is the ability of the apparatus to reach the required input performance. This takes into account the statistical process control and permits a measurement of whether the machine can respect the interval tolerances (defined by the top and bottom targets) given in the specifications. The apparatus concerned in this study is the nuclear press described in previous chapter and the sintered input dimensions of the pellet are given below by: diameter = 8.45 ± 0.09 mm, hole diameter = 2.2 mm and, height < 12 mm. The results of optimization study have been used to calculate size of a new tool. The proportional law is possible for the small gap and the new calculate diameter is 9.370 mm with the high tolerance fixed to ± 0.005 mm. The needle diameter has not been changed. Two new tools have been built, one with needle and one without needle. We decided to shape 400 pellets with each tool. Only hole pellet results are presented in this study. The compaction cycle during 400 annular pellet productions has been realized [17]. The powder volume depends on the weight of the pellet (2.180 g) and the bulk powder density. The volume of the powder necessary to make 400 pellets is 0.689 L. For information, the capacity of the jar is 0.751 L and 0.374 L between the jar and the powder column.

The pellets were shaped in continuous compaction, and a pathway system was built to keep the order and the direction of the pellet. This order was monitored to check the press variations (drift) and direction, and to see the side where the upper punch applied the force. All the compaction cycles were recorded in the press database software. The pellets were put into glass tubes containing 37 pellets (Fig. 2). After compaction, each green pellet was measured by laser profilometer (height, and diameter corresponding to height) and weighed with precision scales. A chronological number was written on the side directly in contact with the upper punch. All the pellets (100 per batch) were then placed in an alumina crucible and sintered in a furnace under air. The sintering conditions were



Fig. 3. Sintered pellets in the alumina container (100 pellets).

1600 °C, with 4 °C/min for the heating up, for a duration set at 4 hours, followed by 2 °C/min for the cooling (Fig. 3). The same measurements were carried out on pellets after sintering (height, diameter and weight) [18].

As shown in the Figure 4, the average diameter of the pellets is 8.510 mm, the maximum and minimum diameters are respectively 8.533 mm and 8.487 mm. The project objective was reached, but the diameter of the die must be reduced because the average diameter is still too high. We found out that the distribution is not centred and the asymmetric coefficient is 0.572. The average is 8.508 mm. The maximum is 8.533 and the minimum is 8.490. The standard deviation is 0.0068 and the variance is 4.75×10^{-5} . The Alfa coefficient of the confidence gap is 0.05. The Cp capability process is 5.03. The performance process coefficients Pp and Ppk are respectively 4.35 and 1.52 and we must conclude that the process is very capable [19].

Table 3 summarizes objectives and results of all studies, the die dimensions of each die calculated with proportionality law.

To better understand the results, the curves in Figure 5 show different experimental and calculation results. It shows the evolution of the pellet height depending on the diameter. The optimization and capability study conclusions are indicated. For each study, you have the green and sintered pellet diameters and the die diameters obtained by the application of the proportionality law (data shown in

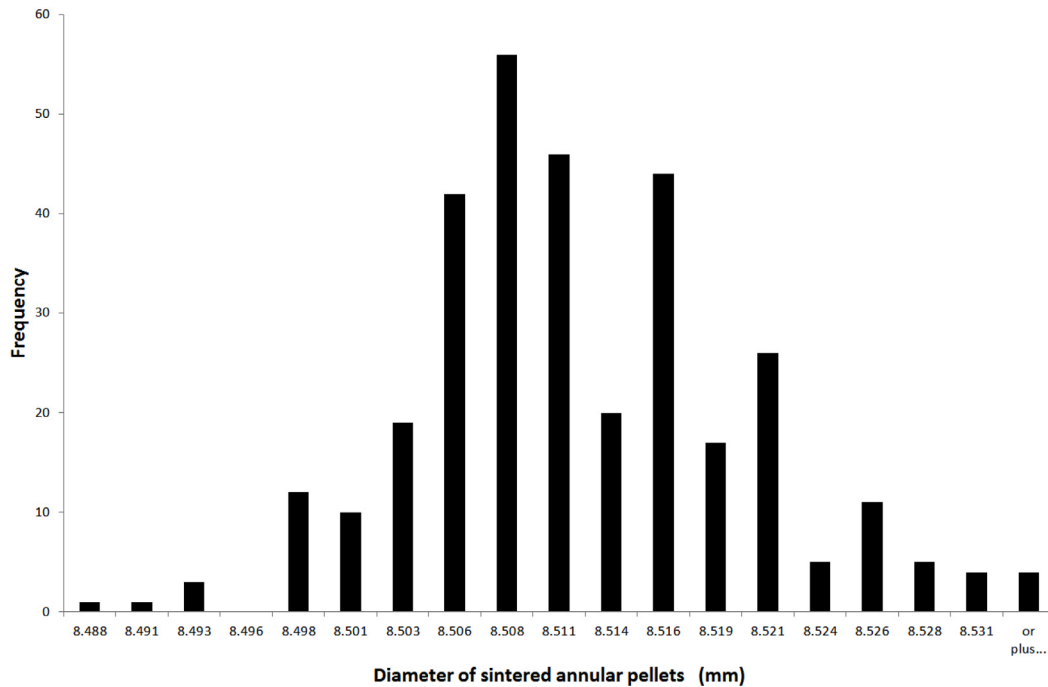


Fig. 4. Histogram of the sintered pellet diameter.

Table 3. Comparison between objective and result diameters, compared to trial number 308.

	Φ_{die} (mm)	$\Phi_{sintered}$ (mm)
Optimization study result	10.000	9.015 ± 0.012
Capability study objective		8.450 ± 0.090
Capability study result	9.370 ± 0.005	8.510 ± 0.023

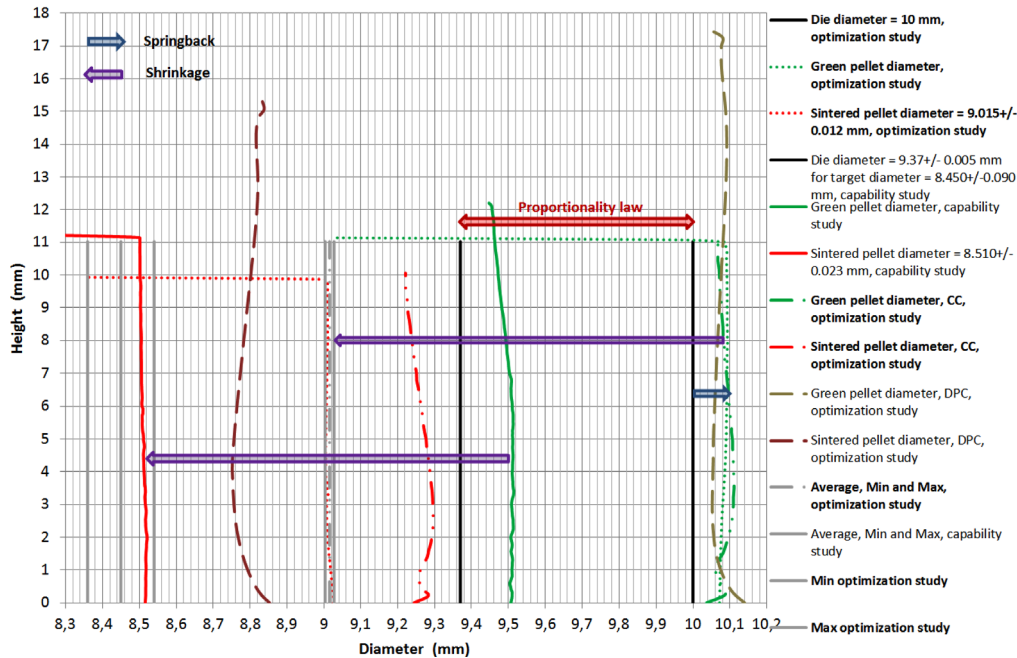


Fig. 5. Comparison between optimization and capability studies, experimental and calculated results.

green for green pellets and red for sintered pellets). We can see the springback between the die and green pellet, as well as shrinkage between green and sintered pellets. Finally, the calculated green and sintered pellet diameters with CC and with DPC models, used for an optimization study without hole and carried out with the Abaqus[®] software are shown. The calculation results show that the model parameters must be optimized. DPC behavior is better than that of CC, as the shape of the sintered pellet is conical. The model behavior at the base of the pellet does not suit the requirements. The height of the sintered pellet must be modified, and the sintered densities are weak. The sintering is too high and must be reduced.

7 Conclusions and perspectives

Producing tomorrow's fuel pellets in a hot cell will require the use of new press technology, due to the nuclear constraints and very strict shape criteria. This publication describes an optimization study on the pressing cycle of the CEA-Champalle electromechanical press, an apparatus which is compact, modular and nuclearized for hot cell operation. It is known that the pressing cycle influences the density gradients in green pellets. In order to predict the diameter tolerance of pellets after sintering, a compaction modelling and simulation program was also undertaken. The density card of the pellet enabled the shrinkage to be calculated and compared to experimental results. With lubricant in the powder and new pellet diameter and tolerance, the capability of the press to manufacture 400 pellets with hole was studied in a mock-up with remote handling. Results showed that the die diameter calculated and the press cycle set enabled pellets to be shaped with satisfactory tolerances. Simulation and associated model-

ling are present in a main goal to be able to anticipate the demanding manufacturing factors, which can influence the press settings before the production cycle, and then during the manufacturing, to be able to have the shortest possible response time to correct parameters to ensure finished products with stable quality. Research into powder compaction behaviour will continue, in order to obtain an improved model response with a new powder and using a discrete element method to better take into account the behaviour between aggregates [20,21].

We would like to thank the Simulia/Abaqus team for their support and in particular C. Geney. Our thanks also to Champalle and all the Process Cycle Advanced Technology Laboratory team.

References

1. I. Aydin, J. Briscoe, Dimensional variation of die pressed ceramic green compacts, comparison of a FEM with experiment, *J. Eur. Ceram. Soc.* **17**, 1201 (1997)
2. P.R. Brewin, O. Coube, P. Doremus, J.H. Tweed, *Modelling of powder die compaction*, Springer Engineering Materials and Processes (Springer-Verlag, London, 2008), p. 57, §4.2.2, p. 59 §4.2.3
3. P. Pizette, C.L. Martin, G. Delette, P. Sornay, F. Sans, Compaction of aggregated ceramic powders: From contact laws to fracture and yield surfaces, *Powder Technol.* **198**, 240 (2010)
4. P. Pizette, C.L. Martin, G. Delette et al., *J. Eur. Ceram. Soc.* **33**, 975 (2013)
5. G. Kerboul, Étude de l'endommagement des produits céramiques crus par émission acoustique, Thèse INSA Lyon, 1992
6. D.D. Zenger, H. Cai, *Handbook of the common cracks in green P/M compacts* (Powder Metallurgy Research Center, WPI, 1997)

7. P. Jonsen, A. Haggblad, Modelling and numerical investigation of the residual stress in a green metal powder body, *Powder Technol.* **155**, 196 (2005)
8. G. Delette, P. Sornay, J. Blancher, A Finite Element modelling of the pressing of nuclear oxide powders to predict the shape of LWR fuel pellet after die compaction and sintering, in *AIEA Technical Committee, Brussels, 20-24 October 2003* (2003)
9. J.-P. Bayle, Minor actinide bearing blanket manufacturing press and associated material studies for compaction cycle optimization, in *NuMat 2014 Nuclear Materials conference, 27-30 October 2014 Clearwater Beach, Florida* (2014)
10. J.-P. Bayle, *Electromechanical press for nuclear compaction in hot cell* (WNE, Paris, 2014)
11. J.-P. Bayle, *Minor actinide bearing blanket manufacturing press* (Hotlab, Baden, 2014)
12. J.-P. Bayle, WO2015/181121A1, Brevet CEA/Champalle, Presse pour mettre en forme des pastilles dans un environnement restreint et hostile et procédé d'assemblage de la presse
13. J.-P. Bayle, Finite element modeling and experiments for shaping nuclear powder pellets, *Procedia Chem.* **7**, 444 (2012)
14. C. Dellis et al., PRECAD, A Computer-Assisted Design and Modelling Tool for Powder Precision Moulding, in *HIP'96 Proceeding of the international conference on Hot Isostatic Pressing, 20-22 May 96 Andover, Massachusetts* (1996) pp. 75-78
15. Abaqus[®] User manual, Vs 6.11 Analysis User's, Manual Volume III: Materials, section 22.3.1, 22.3.2, 22.3.4
16. Cast3 m[®] User manual, Modèle non linéaire, T. Charras, Edition 2011
17. J.-P. Bayle, Modelling of powder die compaction for press cycle optimization, in *TopFuel 2015, Sept. Zurich* (2015)
18. O. Gillia, Modélisation phénoménologique du comportement des matériaux frittants et simulation numérique du frittage industriel de carbure cémenté et d'alumine, Thèse INPG, 2000
19. F. Desnoyer, Memento sur la notion de capabilité, TI, ag1775, versus 10/01/2004
20. E. Remy, *J. Eur. Ceram. Soc.* **32**, 3199 (2012)
21. P. Parant, *Study and modelling of compaction of metal oxide microspheres into pellets* (E-MRS, Warsaw, Poland, 2014)

Cite this article as: Jean-Philippe Bayle, Vincent Reynaud, François Gobin, Christophe Brenneis, Eric Tronche, Cécile Ferry, Vincent Royet, Modelling of powder die compaction for press cycle optimization, *EPJ Nuclear Sci. Technol.* **2**, 25 (2016)